A nonlinear dynamical model of oscillatory zoning in plagioclase

Ivan L'Heureux

Ottawa-Carleton Geoscience Centre, and Department of Physics, University of Ottawa, Ottawa, Ontario K1N 6N5, Canada

Anthony D. Fowler

Ottawa-Carleton Geoscience Centre, and Department of Geology, University of Ottawa, Ottawa, Ontario K1N 6N5, Canada

Abstract

A nonlinear dynamical model for oscillatory zoning found in many plagioclase crystals is presented. This model is based on an isothermal, constitutional, undercooling mechanism involving diffusion and growth kinetics in the melt. A phenomenological effective-partition coefficient, K, which relates the composition in the melt to the composition of the growing crystal, is introduced. A linear stability analysis and direct numerical solutions of the model are presented. It is found that when K is larger than unity, the system evolves to a stable, uniform-growth regime. However, when K is smaller than unity, which is a realistic case for melts of intermediate An composition, the model shows the existence of a Hopf bifurcation leading to oscillatory zoning. As the system is driven further from equilibrium, chaotic solutions occur. The features of these zoning patterns are consistent with those found in nature.

Introduction

Nonlinear dynamics has been applied to a wide variety of physicochemical systems. Typically, these systems are nonlinear because of feedback mechanisms that couple dynamical variables. This coupling often has important effects when the systems are far from equilibrium. For near-equilibrium crystallization of solid solutions, we expect crystals of homogeneous composition. Farther from equilibrium, a variety of different patterns may arise: zoning, dendrites, and spherulites (Lofgren, 1974; Kessler et al., 1988).

Oscillatory-zoned plagioclase crystals are very common in andesites and diorites with plagioclase that is <50 mol% An. The zoning is characterized typically by regular compositional variations superposed onto irregular and sharp discontinuities (e.g., Pearce and Kolisnik, 1990). Recently, Higman and Pearce (1993) analyzed zone thicknesses from many oscillatory-zoned plagioclase crystals, concluding that the data are consistent with a nonlinear deterministic mechanism for zoning.

There have been various nonlinear models proposed to explain the origin of the zoning. Brandeis et al. (1984) modeled oscillatory crystal growth as due to nucleation-induced temperature oscillations. Allègre et al. (1981) considered a model based on diffusion and a relaxation time for the growth rate. Haase et al. (1980) and Ortoleva (1990) proposed a model based on a diffusion mechanism and an autocatalytic reaction scheme. Lasaga (1982) modeled a diffusion-based growth mechanism with physically realistic expressions for the growth rate but did not find oscillating solutions. In this work, we present a model based on the constitutional (isothermal) undercooling mechanism (Rutter and Chalmers, 1953; Tiller et al., 1953; Sibley et al., 1976).

The model

Constitutional undercooling occurs when the liquid in contact with the growing solid front has a composition different from its bulk value. This results in a concentration gradient in the vicinity of the front. The liquidus temperature corresponding to the concentration at the growing front is then locally different from the liquidus temperature of the bulk equilibrium system, and isothermal undercooling is therefore induced. The degree of constitutional undercooling determines the growth rate. The relative magnitudes of the diffusion process and the growth in turn drive the change in concentration at the interface, which affects the degree of undercooling. This interplay in the growth kinetics therefore provides the nonlinear feedback necessary for the existence of nontrivial asymptotic behavior.

Basic equations

Observed compositional zoning is often planar. Thus we assume growth in one spatial dimension, x. As diffusion processes in the solid are orders of magnitude slower than diffusion in the melt, they are neglected.

To describe the growth process, we use a frame of reference, F, comoving with the growing crystal front, with the origin $x = 0$ fixed at the front (Fig. 1). The region $x > 0$ corresponds to the melt. Let F' denote the frame of reference of the crystal, with the origin initially coinciding with the origin of F. The positional coordinate of the growing front in F' is then
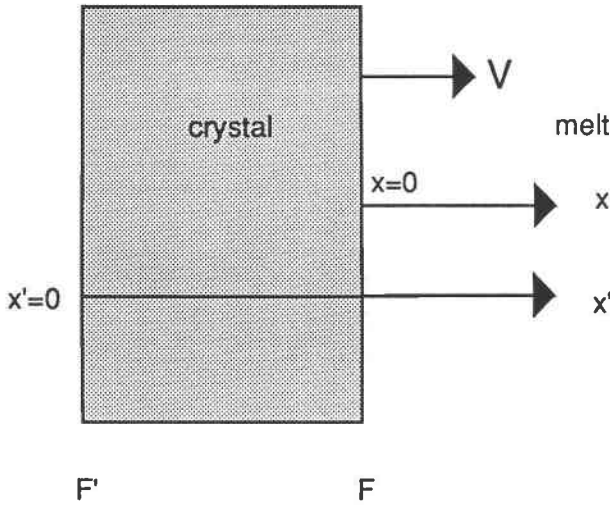
Fig. 1. Schematic diagram of the growing crystal illustrating the reference frames (symbols defined in Table 1).

TABLE 1. List of symbols

a	growth-rate parameter
A	constant defining the effective partition coefficient
b	growth-rate parameter
B	constant defining the effective partition coefficient
$c(x, t)$	concentration of An in the melt
$c(0, t)$	concentration of An in the melt at the growing front
$c_s(0, t)$	concentration of An in the crystal at the growing front
$\hat{c}$	concentration of An in the melt far from the growing front
c_i	initial concentration of An in the melt
c_0	steady-state value of $c(0, t)$
D	diffusion coefficient
G_T	growth-rate velocity derived from kinetic models
K	effective partition coefficient
K_D	constant defining the effective partition coefficient
R	ideal gas constant
R_c	continuous growth factor in G_T
R_s	surface nucleation growth factor in G_T
t	time
T	temperature
T_g	glass-transition temperature
T_L	equilibrium liquidus temperature
U	velocity scale factor in G_T
ν_{An}, ν_{Ab}	molar volume of An and Ab
V	growth rate of the crystallization front
V_0	steady-state value of V
x	positional coordinate in a frame moving with the front
x'	positional coordinate in a frame fixed with the crystal
X	An composition of the melt at the growing front
α	$\sqrt{1 + 4\Gamma D/V_0^2}$
β	$1/\alpha^2$
ΔG	molar Gibbs free-energy difference between crystal and melt
ΔH	molar-enthalpy difference between crystal and melt
ΔH_f	molar enthalpy of fusion
ΔH_m	molar enthalpy of mixing
ΔT	$T_L - T$
Γ	input-flow rate per unit volume
θ	$\dfrac{\hat{c}}{V_0}\dfrac{dV}{dc}$

$$x' = x + \int_0^t V(t') \, dt'$$

where $V(t)$ is the velocity of the front (Table 1). The flux, J, of a crystal component of concentration, $c(x, t)$ (number of moles per unit volume), at position x and time t is then given by

$$J = -D\frac{\partial c}{\partial x} - Vc \tag{1}$$

where D is the diffusion coefficient of the component in the melt. For simplicity, we neglect the concentration and temperature dependence of D. We use the mass continuity equation in the form

$$\frac{\partial c}{\partial t} = -\frac{\partial J}{\partial x} + S$$

where S stands for source terms, which describes the effects of eventual mass sinks or sources. We thus obtain the diffusion equation:

$$\frac{\partial c}{\partial t} = D\frac{\partial^2 c}{\partial x^2} + V\frac{\partial c}{\partial x} - \Gamma(c - \hat{c}). \tag{2}$$

The Γ crudely describes the effect of the source term and corresponds to a mass-input flow rate per unit volume. The Γ can then be interpreted as the inverse of the average residence time of the material component in the reservoir. This considers the possibility that the melt reservoir is an open system, with material input of concentration $\hat{c}$ far from the growing front. In the absence of mass input ($\Gamma = 0$), $\hat{c}$ is simply interpreted as the bulk concentration in the melt far from the growing front.

The initial condition is

$$c(x, 0) = c_i. \tag{3}$$

The concentration far from the growing front is assumed to be equal to the input concentration (or the bulk value in the absence of mass input):

$$c(\infty, t) = \hat{c}. \tag{4}$$

Continuity of the flux at the growing front gives another boundary condition,

$$D\frac{\partial c}{\partial x}\bigg|_0 + [c(0, t) - c_s(0, t)]V = 0 \tag{5}$$

where $c_s(0, t)$ is the interface concentration of the component in the crystal. To close the set of equations, a relation between $c_s(0, t)$ and $c(0, t)$ is needed. The simplest phenomenological relation that can be used is a constant partition coefficient, K:

$$c_s(0, t) = Kc(0, t). \tag{6}$$

For the case where c refers to a major component, other phenomenological relations can be used. For instance, it has been shown that an appropriate relation between the melt and solid-interface concentrations for a two-component system may be written as

$$c_s(0, t) = \frac{K_D B c(0, t)}{A + (K_D - 1)c(0, t)} \tag{7}$$

where A, B, and K_D are approximately constant for a fixed

temperature (Lasaga, 1982). If the concentration $c(0, t)$ does not change appreciably with time, one can define an effective partition coefficient,

$$K = \frac{K_D B}{A + (K_D - 1) \langle c(0, t) \rangle} \quad (8)$$

where $\langle c(0, t) \rangle$ denotes the time average of the concentration (Lasaga, 1982). One then approximately recovers the phenomenological relation given by Equation 6. In the following, we consider a constant K such that the boundary condition at the interface becomes

$$D\frac{\partial c}{\partial x}\bigg|_0 + c(0, t)(1 - K)V = 0. \quad (9)$$

For the plagioclase system in basalts, the equilibrium value of the partition coefficient is larger than unity. However, in view of the interpretation given by Equation 8, we consider the possibility that K may be smaller than unity. Indeed, our calculations based on Equation 7 show $K \approx 1.5$ for plagiocase of composition An_{50} in a typical basaltic melt. However, for An_{33} plagioclase, $K \approx 0.55$ in a typical basaltic melt and $K \approx 0.61$ in a typical andesitic melt.

A more realistic model would consider the energy-conservation equation, with a coupling of the temperature field to the concentration field through the temperature dependence of the diffusion or through the effect of the latent heat released at the crystal front. Actually, the latter coupling is responsible for the oscillatory pattern observed in explosive crystallization (Van Saarloos and Weeks, 1984). However, the heat diffusivity is very different from the matter-diffusion coefficient. Consequently, the length scales for a latent heat-driven crystallization are on the order of centimeters (Brandeis et al., 1984), corresponding to much slower dynamics. Thus an isothermal model constitutes a good approximation for the investigation of small-scale zoning patterns.

Growth rate

To complete the model, the velocity of the growing front is required. This provides the nonlinear feedback necessary for the existence of solutions exhibiting a nontrivial asymptotic behavior. As the growth process is usually slow (<1 μm/s), we assume that the velocity of the growing front relaxes instantaneously to its growth-rate value, $G_T[c(0, t)]$, defined by growth kinetic models (see below) at temperature T:

$$V(t) = G_T[c(0, t)]. \quad (10)$$

A realistic expression for G_T has been established (L'Heureux, 1993) by fitting the laboratory measurements of Kirkpatrick et al. (1979) to the Calvert-Uhlmann growth model (Calvert and Uhlmann, 1972). This model expresses the overall growth rate as a geometric average of two processes: a longitudinal growth, R_s, by surface nucleation and a continuous growth, R_C, responsible for the lateral spread of crystalline layers,

$$G_T = U(R_s R_C^2)^{1/3} \quad (11)$$

where

$$R_s = \exp\left(-\frac{3a}{T\Delta T}\right)\exp\left(-\frac{b}{T - T_g}\right) \quad (12)$$

$$R_C = \left[1 - \exp\left(-\frac{\Delta G}{RT}\right)\right]\exp\left(-\frac{b}{T - T_g}\right). \quad (13)$$

Here, U is a velocity scale, a and b are constants, and ΔT is the undercooling,

$$\Delta T = T_L - T \quad (14)$$

where T_L is the equilibrium liquidus temperature, T_g denotes the ideal glass transition temperature defined as the temperature for which the melt has infinite viscosity because of the vanishing of its configurational entropy, and $\Delta G > 0$ denotes the molar Gibbs free-energy difference between the crystal and the liquid. For small degrees of undercooling, this quantity is conventionally related to ΔT through the relation

$$\Delta G = \Delta H \Delta T / T_L \quad (15)$$

(e.g., Dowty, 1980), where $\Delta H = \Delta H_f + \Delta H_m$ is the molar enthalpy difference between the crystal and the liquid at the liquidus temperature. The latter quantity is expressed as the sum of the molar enthalpy of fusion, ΔH_f, and the molar enthalpy of mixing, ΔH_m. Our approach is similar to Lasaga (1982) and Muncill and Lasaga (1987) but does not require the use of viscosity data.

Finally, the relation between the concentration $c(0, t)$ of An and the An composition (mole fraction) X in the melt at the interface is

$$c(0, t) = \frac{X}{v_{An}X + (1 - X)v_{Ab}} \quad (16)$$

where v_{An} and v_{Ab} are the molar volumes of An and Ab, respectively. As these two molar volumes are nearly equal ($v_{An} = 100.79$ cm³/mol, $v_{Ab} = 100.07$ cm³/mol), a good approximation is

$$c(0, t) = X/v_{An}. \quad (17)$$

Thus, the concentration $c(0, t)$ of An, expressed in units of inverse molar volume, is directly given by the composition X.

Expressions for $T_L(X)$ were taken from Lasaga (1982). Weill et al. (1980) provided $\Delta H_m(X)$ and $T_g(X)$ (approximated as the actual glass-transition temperature). For simplicity, we assume that the enthalpy of fusion, ΔH_f, is given by the sum of the Ab and An pure-component enthalpies of fusion weighted by the composition

$$\Delta H_f(X) = X\Delta H_f^{An} + (1 - X)\Delta H_f^{Ab} \quad (18)$$

where $\Delta H_f^{An} = 19$ kcal/mol (Robie et al., 1978) and $\Delta H_f^{Ab} = 14.26$ kcal/mol (Weill et al., 1980). Other expressions for $\Delta H_f(X)$ could be used, but growth curves are not sensitive to the particular value of ΔH (L'Heureux, 1993).

The functions $\ln U(X)$ [$U(X)$ in cm/min], $a(X)$, and $b(X)$ were fitted to quadratic polynomials:

TABLE 2. Growth-rate parameters

n	u_n	a_n (K²)	b_n (K)
0	−4.0204	1225890	1099.6
1	7.1197	−3509543	2193
2	0	2566582	−2114.3

$$\ln U(X) = \sum_{n=0}^{2} u_n X^n, \; a(X) = \sum_{n=0}^{2} a_n X^n$$

and

$$b(X) = \sum_{n=0}^{2} b_n X^n$$

(Table 2). A good fit to the experimental data was obtained with this model (see L'Heureux, 1993). Recent measurements of growth velocity at low An concentrations (Muncill and Lasaga, 1987) are also consistent with this analytical expression. The main terms defining the shape of the growth curve as a function of c (or X) are $U(X)$ and $T_L(X)$. The growth curves depend only slightly on $a(X)$, $b(X)$, $T_g(X)$, and $\Delta H(X)$. As shown in Figure 2, the calculated growth velocity is a strongly increasing function of the concentration.

In summary, Equations 2, 3, 4, 9, and 10 describe the model considered here. The governing parameters are D, Γ, T, $\hat{c}$, and K.

RESULTS

In the following, we use a value of the diffusion coefficient between 10^{-11} and 10^{-10} m²/s (Maaløe, 1985). The value of Γ may be estimated on the basis of typical magma chamber volumes and volcanic-eruption rates. We use data from the Hawaiian volcanoes (Decker et al., 1987), as their properties are relatively well known: $\Gamma \approx 10^{-11}$/s.

Stability analysis

By setting the left side of Equation 2 to 0, solving for the steady-state growth velocity, V_0, and concentration, c_0, is straightforward:

$$V_0 = 2\sqrt{\Gamma D}\left\{\left[1 - 2K + 2\frac{(1 - K)\hat{c}}{c_0 - \hat{c}}\right]^2 - 1\right\}^{-1/2} \quad (19)$$

$$c_0 = \hat{c}\frac{1 + \alpha}{2K + \alpha - 1} \quad (20)$$

where $\alpha = \sqrt{1 + 4\Gamma D/V_0^2}$. A linear-stability analysis about this steady-state solution (L'Heureux, 1993) allows the time evolution (growth or decay) of a small perturbation about the steady state to be investigated. The analysis showed that, when $K > 1$, the steady state is stable; no asymptotic oscillatory behavior is possible. This confirms the numerical findings of Lasaga (1982).

On the other hand, when K is smaller than unity, the dynamics are more complicated (Fig. 3). The axes on this
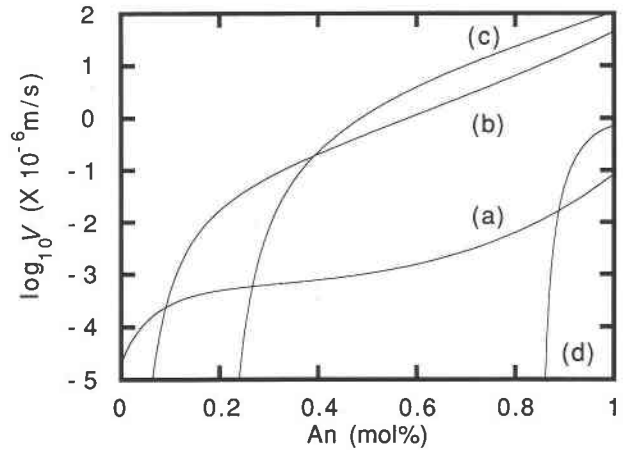
Fig. 2. Behavior of the growth velocity, $V = G_T$, as a function of An content for various temperatures: (a) $T = 1200$ K; (b) $T = 1400$ K; (c) $T = 1600$ K; (d) $T = 1800$ K. See Eqs. 11–13.

diagram are the dimensionless slope of the growth curve

$$\theta = \frac{\hat{c}}{V_0}\frac{dV}{dc} \quad (21)$$

and a parameter related to Γ,

$$\beta = \alpha^{-2} = 1/(1 + 4\Gamma D/V_0^2). \quad (22)$$

In region A, the steady state is stable, but damped oscillations are possible. As the system moves from region A to region B, it undergoes a Hopf bifurcation. This signifies that the steady state loses stability at a critical value of the governing parameter, θ, and is replaced by a periodic solution. Oscillatory zoning is therefore possible near the Hopf bifurcation line. As the system approaches region C from lower values of θ, it may undergo further instabilities. However, the nature of these instabilities is not determined by the linear stability analysis summarized here, as it pertains to the steady state only. In region C, the steady state is unstable without oscillation. In region D, the steady state is stable and does not support any damped oscillation. Finally, in region E, the linear stability analysis does not give a solution.

Numerical solutions

To verify these findings and to investigate the nature of the linearly unstable solutions, a numerical analysis of the model was also made by L'Heureux (1993). The scheme is convergent and stable over a wide range of parameter values. As further verification, the numerical solution for the linear problem $V = $ constant and $\Gamma = 0$ agrees with the known analytical solution (Eq. 10 of Smith et al., 1955).

Figure 4a–4c extends the work of L'Heureux (1993) and gives the concentration of An in the solid as a function of the distance from the core of the crystal for various parameter values. These figures are typical, and other parameter values give the same overall behavior. When
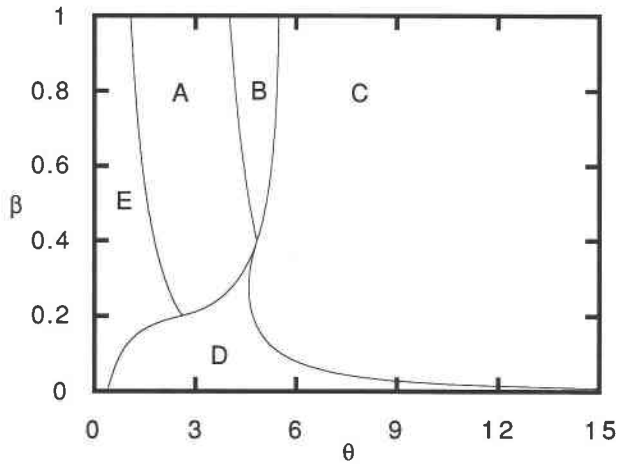
Fig. 3. Stability diagram showing the behavior of the steady state according to a linear stability analysis for $K = 0.63$ (for other choices of $K < 1$, the stability diagrams are qualitatively similar). See text for an explanation of the stability fields.

$K > 1$ (Fig. 4a), the solution approaches the (stable) steady state without oscillation, in accordance with the stability analysis of the previous section. In Figure 4b and 4c, the effective partition constant is smaller than unity ($K = 0.63$), and $\hat{c}$ is varied. Figure 4b corresponds to a point in region A of the stability diagram of Figure 3. As expected from the stability analysis, the solution has an oscillatory character as it approaches the stable steady state. Figure 4c corresponds to a point in region B of the stability diagram, where the steady state is unstable. In this instance, the model corresponds to a point in the stability diagram located just beyond the Hopf bifurcation line where a periodic solution is expected. This is indeed the case. The distance between the peaks in the signal is $5.29D/V_0 = 390$ μm. Because V_0 is quite insensitive to the value of D in the range of interest, this spatial periodicity corresponds to 39–390 μm for $D = 10^{-11}$–10^{-10} m^2/s, respectively. This value (particularly for the lower values of D) is consistent with typical observations of compositional zoning in plagioclase.

Figure 5 shows typical patterns for a different temperature ($T = 1400$ K) and $K = 0.55$. In Figure 5a, the model corresponds to a point in the stability diagram that is just beyond the Hopf bifurcation line in region B of Figure 3. The solution shows an oscillatory behavior, leading to an average distance between peaks that is equal to 46–460 μm for $D = 10^{-11}$–10^{-10} m^2/s, respectively.

Finally, Figure 5b shows the dynamics after $\hat{c}$ was further increased with respect to the value of Figure 5a. This has the effect of shifting the system further to the right of the Hopf bifurcation line of the corresponding stability diagram while keeping the stable point in region B of Figure 3. We see that the solution has developed an irregular, chaotic behavior. It should be noted that, in this last instance, the peak values of the numerically obtained melt concentration were sometimes slightly higher than 1. This problem should not arise with a more exact ex-
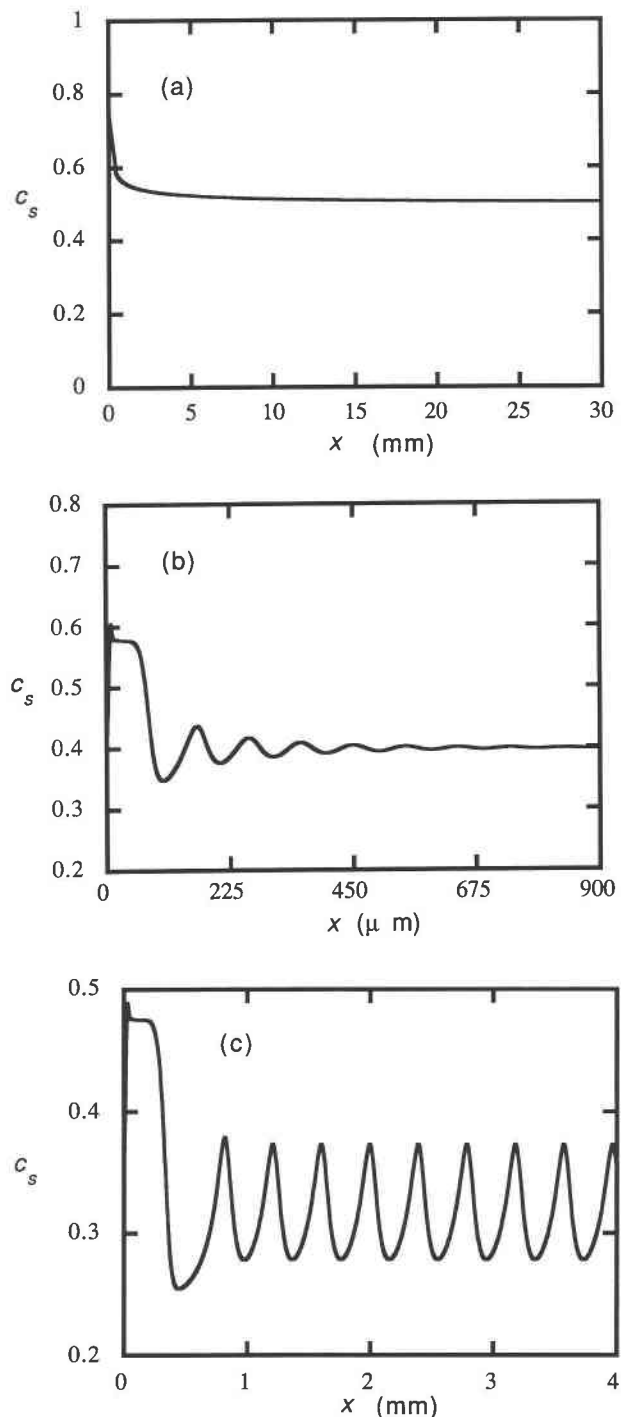
Fig. 4. Numerical solution for the An concentration in the crystal, $c_s(0, t)$, at the growing front as a function of the distance from the core $x' = \int_0^t V(t')\,dt'$. $D = 10^{-10}$ m^2/s, $\Gamma = 10^{-11}$/s, and $T = 1600$ K. (a) $K = 1.5$, $\hat{c} = 0.5$, $c_i = 0.5$ ($V_0 = 0.0362$ μm/s); (b) $K = 0.63$, $\hat{c} = 0.40$, $c_i = 0.6$ ($V_0 = 5.566$ μm/s); (c) $K = 0.63$, $\hat{c} = 0.32$, $c_i = 0.5$ ($V_0 = 1.343$ μm/s).
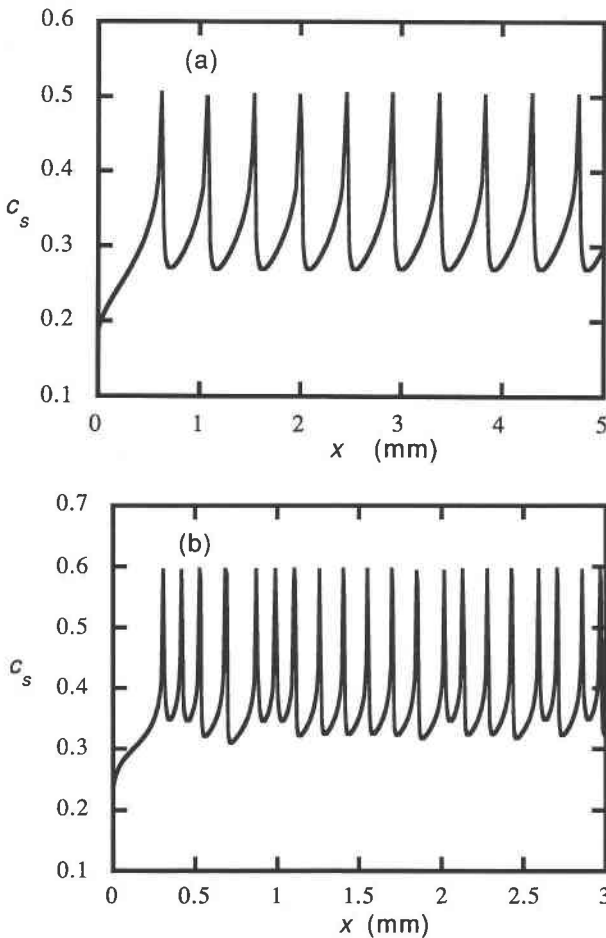
Fig. 5. As in Fig. 4 but $T = 1400$ K and $K = 0.55$; (a) $\hat{c} = c_i$ = 0.33 ($V_0 = 1.158$ μm/s), (b) $\hat{c} = c_i = 0.416$ ($V_0 = 4.402$ μm/s).

pression for the growth rate, particularly at higher undercoolings.

DISCUSSION

Zoning features

We compare the results of the model with known features of oscillatory-zoned plagioclase. Zoning tends to be very diverse within individual crystals and among crystals of the same sample, so that it is difficult to classify the zoning features. Nevertheless, some general characteristics can be identified. Oscillatory-zoned plagioclase commonly has zone widths ranging from 1 to 100 μm and amplitudes of 1–40 mol% An. The An content (lower base line of Pearce and Kolisnik, 1990) may remain constant over a zoned interval or decrease with distance outward from the crystal core (Pearce et al., 1987). The oscillations have an asymmetric sawtooth shape with respect to distance. In addition, the oscillating patterns in the crystals are often interrupted by a change in the mode of oscillations or another style of crystal growth (e.g., Pearce and Kolisnik, 1990).

In our model, the wavelengths range from ~40 to ~500 μm, depending on the value of D, T, and K. The lower values accord well with those found in nature. The dependence of the wavelength on D is approximately linear, and this effect is discussed below. Results of several simulations show that model amplitudes are consistent with those found in nature. Because the model does not incorporate explicit variations in temperature or bulk concentration, the steady state is invariant. Consequently, the simulations have no base-line shift in An content.

Note that the shape of the simulated profiles is also an asymmetric sawtooth pattern. Several simulations indicate that the degree of asymmetry is determined mainly by temperature. For larger undercoolings, the system is further from the equilibrium, and the degree of asymmetry increases (Figs. 4c and 5a). The individual peaks are characterized by a smooth rise to higher An content followed by a rather sharp drop. This is in contrast to the interpretation of Pearce and Kolisnik (1990), which depicts a sharp rise followed by a smooth decay. On the basis of the physical model of constitutional undercooling, we expect the type of pattern exhibited by our simulations; it corresponds to a progressive buildup of rejected solute at the crystal interface driven by fast growth and sluggish diffusion. The increase in concentration generates a strong gradient so that diffusion eventually dominates the process, resulting in a sudden decrease of the interface concentration. This discrepancy in peak shape may be resolved by the collection of more empirical data or, alternatively, by the introduction of other physicochemical processes into the model.

The diversity of zoning patterns that arises in nature may be due to large scale effects (e.g., eruptions), in addition to nonlinear, microscopic effects. Recall from Figure 5b that the dynamical behavior may be very rich and include chaos; inspection suggests that it is possible to have sudden and irregular shifts in the zoning patterns, as is observed (Pearce and Kolisnik, 1990). We expect irregular zoning to be chaotic in the sense that the correlation between crystal zone thicknesses decay with distance (e.g., Bergé et al., 1984). However, we caution that the interplay of small, large-scale, and random events may render the detection of chaos difficult. Another causative factor of pattern diversity may be the existence of random fluctuations in the governing parameters. These may stochastically drive the system such that various modes of oscillation may be selected in an unpredictable fashion. The study of such noise-induced transitions (e.g., Horsthemke and Lefever, 1984) is the subject of continuing investigation.

Effects of the governing parameters

Varying critical model parameters on the system dynamics has several effects. Oscillatory behavior may occur when $K < 1$; $K = 1.5$ for An_{50} plagioclase, and $K = 0.55$ for An_{33} plagioclase within a typical basaltic melt, whereas $K = 0.61$ for An_{33} plagioclase in a typical andesitic melt. This is consistent with the idea that oscillatory

zoning is most prevalent in intermediate systems (andesites and diorites) containing plagioclase of approximately An_{30}.

The wavelength of the oscillating pattern approximately scales linearly with the diffusion coefficient, D. Smaller wavelengths are obtained if D values are reduced (e.g., 10^{-12} m^2/s).

An increase in Γ leads to a decrease in the parameter β (see Eq. 22), thus narrowing the window of the existence of oscillating solutions (Fig. 3). However, for geologic conditions, β is very close to 1, and thus the effect of the introduction of new material is negligible.

Our calculations indicate that the range of $\hat{c}$ for which oscillatory behavior may be observed is relatively large (e.g., $\approx 0.30 \pm 0.05$ An mole fraction for $K = 0.63$ at $T = 1600$ K). As the undercooling increases, the domain of existence of oscillatory behavior corresponds to slightly higher $\hat{c}$ values (e.g., $\approx 0.35 \pm 0.05$ An mole fraction for $K = 0.55$ for $T < 1600$ K). However, the oscillatory regime strongly depends on K and hence on the geochemistry and average composition of the system.

An extension of this model that includes a relaxation time between the actual growth rate, V, and its nonequilibrium kinetic value, G_T, was considered by L'Heureux (1993). Linear stability analysis shows that, for $K > 1$, the steady state is still stable, but damped oscillations are possible, in agreement with the findings of Brandeis et al. (1984) and Allègre et al. (1981).

REFERENCES CITED

Allègre, C.J., Provost, A., and Jaupart, C. (1981) Oscillatory zoning: A pathological case of crystal growth. Nature, 294, 223–228.

Bergé, P., Pomeau, Y., and Vidal, C. (1984) Order within chaos: Towards a deterministic approach to turbulence, 329 p. Hermann, Paris.

Brandeis, G., Jaupart, C., and Allègre, C.J. (1984) Nucleation, crystal growth and the thermal regime of cooling magmas. Journal of Geophysical Research, 89, 10161–10177.

Calvert, P.D., and Uhlmann, D.R. (1972) Surface nucleation growth theory for the large and small crystal cases and the significance of transient nucleation. Journal of Crystal Growth, 12, 291–296.

Decker, R.W., Wright, T.L., and Stauffer, P.H. (1987) Volcanism in Hawaii, vols. 1 and 2, 1667 p. U.S. Government Printing Office, Washington, DC.

Dowty, E. (1980) Crystal growth and nucleation theory and the numerical simulation of igneous crystallization. In R.B. Hargraves, Ed., Physics of magmatic processes, p. 419–485. Princeton University Press, Princeton, New Jersey.

Haase, C.S., Chadam, J., Feinn, D., and Ortoleva, P. (1980) Oscillatory zoning in plagioclase feldspar. Science, 209, 272–274.

Higman, S.L., and Pearce, T.H. (1993) Spatiotemporal dynamics in oscillatory zoned magmatic plagioclase. Geophysical Research Letters, 20, 1935–1938.

Horsthemke, W., and Lefever, R. (1984) Noise-induced transitions: Theory and applications in physics, chemistry and biology, 318 p. Springer-Verlag, Berlin.

Kessler, D., Koplik, J., and Levine, H. (1988) Pattern selection in fingered growth phenomena. Advances in Physics, 37, 255–339.

Kirkpatrick, R.J., Klein, L., Uhlmann, D.R., and Hays, J.F. (1979) Rates and processes of crystal growth in the system anorthite-albite. Journal of Geophysical Research, 84, 3671–3676.

Lasaga, A.C. (1982) Toward a master equation in crystal growth. American Journal of Science, 282, 1264–1288.

L'Heureux, I. (1993) Oscillatory zoning in crystal growth: A constitutional undercooling mechanism. Physical Review E, 48, 4460–4469.

Lofgren, G.E. (1974) An experimental study of plagioclase crystal morphology: Isothermal crystallization. American Journal of Science, 274, 243–273.

Maaløe, S. (1985) Principles of igneous petrology, 374 p. Springer-Verlag, Berlin.

Muncill, G.E., and Lasaga, A.C. (1987) Crystal-growth kinetics of plagioclase in igneous systems: One-atmosphere experiments and application of a simplified growth model. American Mineralogist, 72, 299–311.

Ortoleva, P. (1990) Role of attachment kinetic feedback in the oscillatory zoning of crystals grown from melts. Earth-Science Reviews, 29, 3–8.

Pearce, T.H., and Kolisnik, A.M. (1990) Observations of plagioclase zoning using interference imaging. Earth-Science Reviews, 29, 9–26.

Pearce, T.H., Russel, J.K., and Wolfson, I. (1987) Laser-interference and Nomarski interference imaging of zoning profiles in plagioclase phenocrysts from the May 18, 1980, eruption of Mount St. Helens, Washington. American Mineralogist, 72, 1131–1143.

Robie, R.A., Hemingway, B.S., and Fisher, J.R. (1978) Thermodynamic properties of minerals and related substances at 298.15 K and 1 bar (10^5 pascals), pressure and at higher temperatures, 456 p. U.S. Geological Survey, Washington, DC.

Rutter, J.W., and Chalmers, B. (1953) A prismatic substructure formed during solidification of metals. Canadian Journal of Physics, 31, 15–39.

Sibley, D.F., Vogel, T.A., Walker, B.M., and Byerly, G. (1976) The origin of oscillatory zoning in plagioclase: A diffusion and growth controlled model. American Journal of Science, 276, 275–284.

Smith, V.G., Tiller, W.A., and Rutter, J.W. (1955) A mathematical analysis of solute redistribution during solidification. Canadian Journal of Physics, 33, 723–745.

Tiller, W.A., Jackson, K.A., Rutter, J.W., and Chalmers, B. (1953) The redistribution of solute atoms during the solidification of metals. Acta Metallurgica, 1, 428–437.

Van Saarloos, W., and Weeks, J.D. (1984) Surface undulations in explosive crystallization: A nonlinear analysis of a thermal instability. Physica, 12D, 279–294.

Weill, D.F., Hon, R., and Navrotsky, A. (1980) The igneous system $CaMgSi_2O_6$-$CaAl_2Si_2O_8$-$NaAlSi_3O_8$: Variations on a classic theme by Bowen. In R.B. Hargraves, Ed., Physics of magmatic processes, p. 49–92. Princeton University Press, Princeton, New Jersey.